

Phospholipid Nanosomes

Trevor P. Castor*

Aphios Corporation, 3-E Gill Street, Woburn, MA 01801, USA

Abstract: Phospholipid nanosomes are small, uniform liposomes manufactured utilizing supercritical fluid technologies. Supercritical fluids are first used to solvate phospholipid raw materials, and then decompressed to form phospholipid nanosomes that can encapsulate hydrophilic molecules such as proteins and nucleic acids. Hydrophobic therapeutics are co-solvated with phospholipid raw materials in supercritical fluids that, when decompressed, form phospholipid nanosomes encapsulating these drugs in their lipid bilayers. Mathematical modeling and semi-empirical experiments indicate that the size and character of phospholipid nanosomes depend on the several process parameters and material properties including the size and design of decompression nozzle, bubble size, pressure and the rate of decompression, interfacial forces, charge distribution and the nature of compound being encapsulated. Examples are presented for the encapsulation of a protein and hydrophobic drugs. *In vitro* and *in vivo* data on breast cancer cells and xenografts in nude mice indicate that paclitaxel nanosomes are less toxic and much more effective than paclitaxel in Cremophor EL (Taxol). Camptothecin nanosomes demonstrate that the normally very water-insoluble camptothecin can be formulated in a biocompatible aqueous medium while retaining *in vivo* efficacy against lymphoma xenografts in nude mice. *In vitro* data for betulinic acid nanosomes demonstrate enhanced efficacy against HIV-1 (EC₅₀ of 1.01 µg/ml versus 6.72 µg/ml for neat betulinic acid). Phospholipid nanosomes may find utility in the enhanced delivery of hydrophilic drugs such as recombinant proteins and nucleic acid as well as hydrophobic anticancer and anti-HIV drugs.

PHOSPHOLIPID NANOSOMES

Phospholipid nanosomes are small, uniform liposomes manufactured utilizing supercritical fluid technologies. They are nanometer-sized vesicles of phospholipid bilayers comprised of single or multiple lipid bilayers. As such, they are non-toxic, non-antigenic and biodegradable in character since they have the molecular characteristics of mammalian cell membranes. Hydrophilic compounds and therapeutics such as recombinant proteins are encapsulated in the aqueous core while hydrophobic compounds and therapeutics such as anticancer and other water-insoluble drugs are trapped within the lipid bilayers. Encapsulation masks the hydrophobic (water-insoluble) nature of drugs, and permits aqueous, biocompatible formulations to be administered. Phospholipid nanosomes protect the encapsulated therapeutics prolonging their circulation and increasing half-life. For cancer chemotherapy, this increases the likelihood that the drug will reach and destroy cancer cells. Encapsulation also protects cells from the circulating therapeutics and reduces their toxicities.

SUPERCritical FLUIDS

Supercritical fluids preferentially utilized for the manufacturing of phospholipid nanosomes are normally gases such as carbon dioxide, fluorocarbons and alkanes at ambient conditions. When compressed, these gases become dense phase fluids that exhibit enhanced thermodynamic properties of solvation, selection, penetration and expansion. As shown by the pressure-temperature diagram in (Fig. 1), a pure compound enters its supercritical fluid region at conditions that

equal or exceed both its critical temperature and critical pressure. These critical parameters are intrinsic thermodynamic properties of all sufficiently stable pure component compounds. Carbon dioxide, for example, becomes supercritical at conditions that equal or exceed its critical temperature of 31.1°C and its critical pressure of 7.38 Megapascals (MPa).

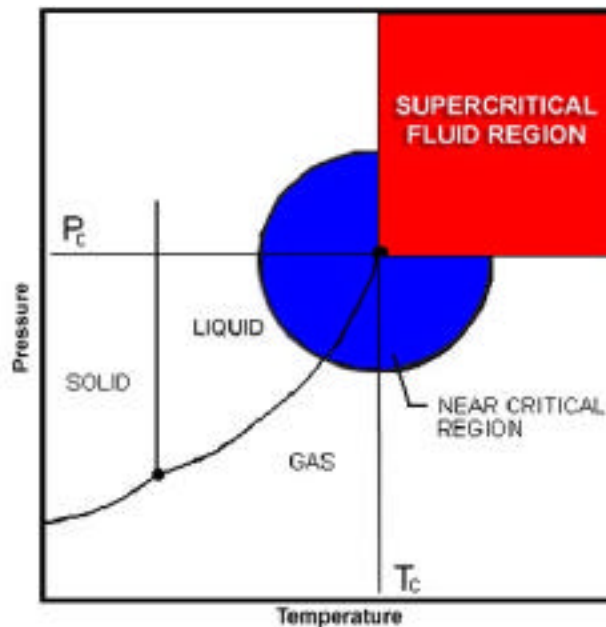


Fig. (1). Supercritical Fluid Phase Diagram

In the supercritical or near-critical fluid region, normally gaseous substances, such as carbon dioxide, become dense phase fluids that have been observed to exhibit greatly en-

*Address correspondence to this author at the Aphios Corporation, 3-E Gill Street, Woburn, MA 01801, USA; Tel: (001) 781-932-6933; Fax: (001) 781-932-6865; E-mail: tcastor@aphios.com

hanced solvation power as compared to the gaseous state. At a pressure of 21 MPa and a temperature of 40°C, carbon dioxide has a density around 0.85 g/ml and behaves very much like a nonpolar organic solvent such as hexane.

A supercritical fluid uniquely displays a wide spectrum of solvation power because its density is strongly dependent on both temperature and pressure - temperature changes of tens of degrees or pressure changes by tens of atmospheres can change solubility by an order of magnitude or more. This unique feature facilitates solute recovery, the "fine-tuning" of solvation power and the fractionation of mixed solutes. The selectivity of nonpolar near-critical or supercritical fluid solvents can be further enhanced by the use of small concentrations of polar entrainers or cosolvents such as ethanol, methanol or acetone. In addition to its unique solubilization characteristics, a supercritical fluid possesses other physico-chemical properties that add to its attractiveness as a solvent. A supercritical fluid solvent can exhibit a liquid-like density and, at the same time, gas-like properties of viscosity and diffusivity. The latter increases mass transfer rates, significantly reducing processing times. Additionally, the ultra-low surface tension of a supercritical fluid allows facile penetration into microporous materials, increasing extraction efficiency and overall yields. Supercritical fluids, critical or near-critical solvents with/without cosolvents are jointly referred to as *SuperFluids* [SFS].

SUPERFLUIDS PHOSPHOLIPID NANOSOMES MANUFACTURING PROCESS

In the *SuperFluids* phospholipid nanosomes (SFS-CFN) manufacturing process [1-3], SFS at appropriate conditions of pressure and temperature are utilized to solvate phospholipids, cholesterol and other nanosomal raw materials in an apparatus such as that shown in the (Fig. 2). The ability of a selected SFS at certain conditions of temperature and pressure to dissolve the nanosomal raw materials is a key ingredient in the process. This selection is thus an important process parameter. A circulation pump is utilized to ensure good mixing between the SFS and nanosomal raw materials in an upper high-pressure loop. After a specific residence time, the resulting mixture is decompressed via a backpressure regulator (valve) through a dip tube with a nozzle into a decompression chamber (vessel B) that contains phosphate-buffered saline or other biocompatible solution.

Bubbles will form at the injection nozzle tip because of SFS depressurization and phase-conversion into a gas, and the solvated phospholipids will deposit out at the phase boundary of the aqueous bubble. As the bubbles detach from the nozzle into the aqueous solution, they rupture causing bilayers of phospholipids to peel off, encapsulating solute molecules and spontaneously sealing themselves to form phospholipid nanosomes. This SFS-CFN injection technique is ideally suited for the nanosomal encapsulation of recombinant proteins for enhanced drug delivery, DNA used in gene therapy, RNAi delivery, and other hydrophilic therapeutics and solutes.

In a second SFS-CFN technique, the phospholipids and the target compound are solvated simultaneously in a SFS "cocktail," which is dispersed continuously into an aqueous environment. The process stream is decompressed, and the

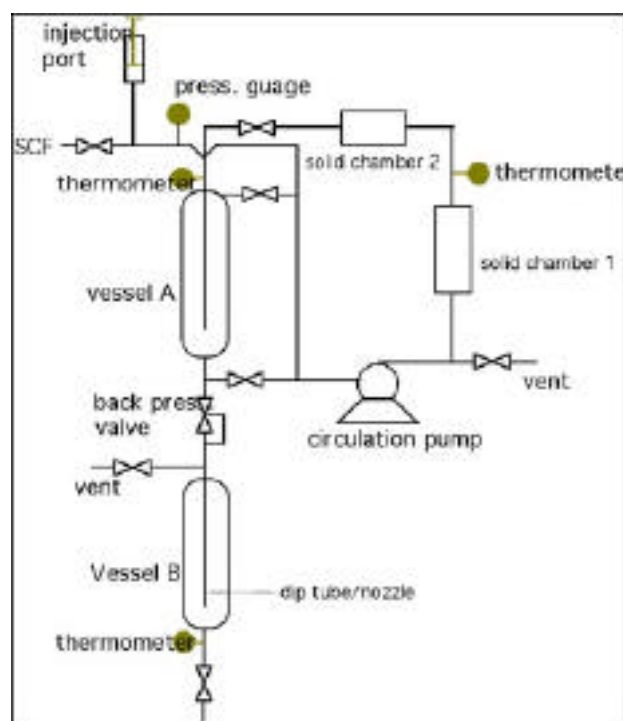


Fig. (2). *SuperFluids* CFN Apparatus

unstable phospholipid bilayer fragments collide and rapidly seal to form nanosomes, entrapping the target compound. The controlling parameters for this process are pressure and rate of decompression. The decompression technique is readily scaled to larger production volumes. It is a "one-step" process, and the SFS stream composition can be designed to achieve concentrated phospholipid and target compound feed streams. The results are high trapping efficiencies and concentrated product recovery streams in the SFS-CFN decompression technique.

In a third technique, SFS-CFN evaporation can be uniquely utilized to encapsulate very hydrophobic molecules such as the potent anticancer drug paclitaxel, camptothecin, a very effective topoisomerase-I inhibitor, and other anticancer and anti-HIV therapeutics such as betulinic acid and bryostatin 1. In this technique, the hydrophobic drug(s) and the phospholipids are directly solvated in the SFS prior to injection into a phosphate-buffered saline or other biocompatible solution. After decompression through a nozzle, the SFS evaporates off leaving an aqueous solution of nanosomes entrapping hydrophobic molecules within their lipid bilayers.

SUPERFLUIDS CFN EQUIPMENT

The SFS-CFN equipment shown in (Fig. 3) consists of three major components or modules: (1) a high-pressure feed system; (2) a high pressure circulation system for mixing and solubilizing the nanosomal raw materials (and in some cases, hydrophobic therapeutics) into the SFS; and (3) a decompression module for reducing the pressure to form the nanosomes and separate the SFS from the nanosomal product.

The first module consists of three high-pressure syringe pumps, one each for the supercritical fluid, cosolvent and

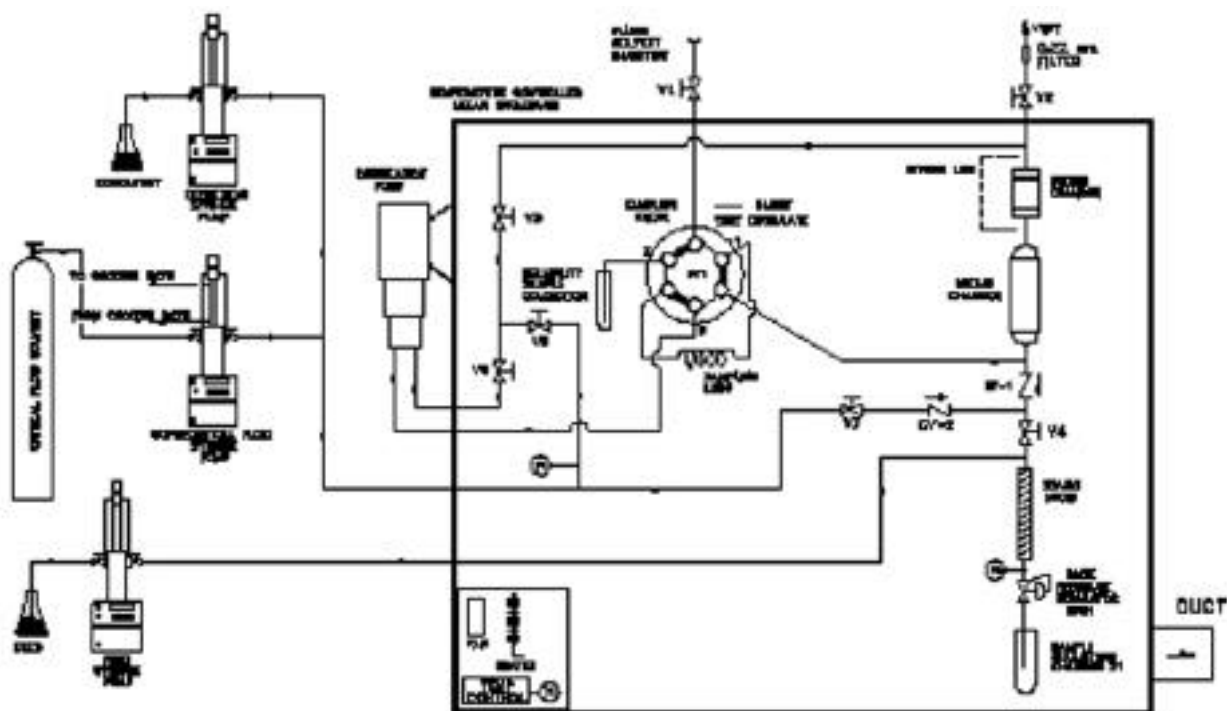


Fig. (3). Process Flow Diagram of *SuperFluids* CFN Laboratory Prototype

product feed. These high-pressure pumps are precision syringe, positive-displacement pumps in which the flowrate can be controlled to 0.1 ml/min. The pumps are rated for a maximum flowrate of 100 ml/min and a maximum pressure of 50 MPa. The pumps can be operated in a constant pressure or constant flowrate mode and can be programmed to operate in fixed and/or step-wise ratios by an internal computer.

The second module consists of a high pressure circulation pump, a Valco sampling valve and 500 µl loop, solids and mixing chambers, a high-pressure circulation loop and an in-line static mixer. The circulation pump is used to circulate the SFS through the solids chamber that can be utilized to contain nanosomal raw materials (hydrophobic therapeutics). The Valco sampling valve can be utilized to sample the SFS stream to determine the best conditions and time for solubilizing the nanosomal raw materials and hydrophobic therapeutics.

The third module consists of an expansion device (back-pressure regulator) and a sample collection chamber. The operating pressure of the system can be preset at a precise level via a computerized controller, which is part of the syringe pumps. Temperature control in the system is achieved by enclosing the apparatus in a 0.64 cm thick Lexan container while utilizing a heater/chiller coupled with a heat exchanger to maintain uniform temperature throughout the system. The container is vented into an organic fume hood or a Biosafety cabinet. The Lexan container also acts as a safety cabinet to contain any accidental pressure release.

The apparatus shown in Figure 3 can be operated in several different modes. In the primary mode (A), the nanosomal raw materials (phospholipids and cholesterol) are placed

within glass wool layers in the solid chamber in order to increase contact between the solid phase and the *SuperFluids* phase and to minimize mass transfer resistance. With V3 and V6 open, and V4 and V7 closed, the high-pressure circulation loop is then pressurized with supercritical fluid and co-solvent via valve V5 (opened) to a pre-specified pressure and temperature. V5 is then closed and the circulation pump turned on for a pre-specified mixing time, usually 60 minutes. During this period, the high-pressure circulation loop can be sampled via the Valco sampling valve SVI and the 500 µl sampling loop. After sampling, the sampling loop is flushed via valve V1 with an appropriate solvent such as ethanol, methanol or acetone. The recovered solutions can be then analyzed to determine the solubility and the amount of nanosomal raw materials in the *SuperFluids* stream at the specified temperature and pressure. The injection pumps are then changed from the constant pressure mode to the constant flow rate mode. Supply valve V5 and exit valve V4 are then opened simultaneously, allowing steady-state discharge of a nanosomal raw materials-enriched *SuperFluids* stream into the sample collection chamber, S1, that contains the target compound in a biocompatible solvent as well as steady state-flow of fresh supercritical fluid and co-solvent into the high-pressure circulation loop. The rate of discharge of the nanosomal raw materials-enriched *SuperFluids* is controlled by the inflow rate of the supercritical fluid and co-solvent. The pressure in the system is kept constant by the backpressure regulator, BPR1.

In operating mode B, the target compound can be placed in the solids chamber with the nanosomal raw materials for cases of hydrophobic compounds that can be directly solubilized in the SFS stream. Alternatively, the target compound can be placed in a second solids chamber that is preferably

downstream of the nanosomal raw materials solids chamber. In operating mode C, with the nanosomal raw materials in the solids chamber, the target compound can be first solvated in a biocompatible solvent such as ethanol and continuously fed via a third syringe pump (feed syringe pump) to meet the nanosomal raw materials-enriched stream just downstream of V4 and upstream of the static in-line mixer. This is a preferred technique for ethanol-soluble anticancer compounds and proteins such as insulin.

In operating mode D, the circulation loop can be inactivated, and the supercritical fluid and cosolvent can be routed through the solids and mixing chambers, through the static in-line mixer and into the collection chamber by opening V5, V3 and V4. The target compound can be continuously fed via the feed syringe pump to meet the nanosomal raw materials-enriched stream just downstream of V4 and upstream of the static in-line mixer. Alternatively, in operating mode E, the nanosomal raw materials-enriched stream can be discharged directly into the sample collection chamber, S1, which contains the target compound in a biocompatible solvent.

In operating mode F, the nanosomal raw materials can be dissolved in the co-solvent and mixed with the supercritical fluid stream just upstream of the static in-line mixer. In this case, both the high-pressure circulation loop and the solids and mixing chambers are bypassed. The target compound can be continuously fed via the feed syringe pump to meet the nanosomal raw materials-enriched stream just upstream of the static in-line mixer. Alternatively, in operating mode G, the nanosomal raw materials-enriched stream can be discharged directly into the sample collection chamber, S1, which contains the target compound in a biocompatible solvent.

SUPERFLUIDS TYPE AND PROPERTIES

The thermodynamic properties of supercritical, critical and near-critical fluids [4] that can be utilized in making phospholipid nanosomes are listed in Table 1.

Carbon dioxide has a very modest critical point, is inexpensive, non-toxic, non-flammable and, for the most part, environmentally acceptable. Nitrous oxide, with the same molecular weight of carbon dioxide is slight polar, a property that helps solubilization of intermediate polarity compounds such as phospholipids and some small molecule therapeutics, and has modest critical points. Nitrous oxide, sometimes used as an oxidant in combustion processes, could lead to undesirable lipid peroxidation. Near-critical propane is also a good solvent for phospholipids and certain therapeutics because of its alkane structure and slight polarity -- factors that contribute to its solvation selectivity in the presence of appropriate cosolvents. Octafluoropropane is a nonflammable alternate to propane. Other alkanes and alkenes such as ethane and ethylene are potential candidates because of their structural similarity with the hydrocarbon chains of phospholipids and their lower critical temperatures. Freon-22 is a good solvent for phospholipids and certain therapeutics because of its large dipole moment (1.4 Debyes). Freon-22, however, has an ozone depletion factor of 0.05 attributed to the chlorine component of the molecule and is being phased out of use and production by environmental concerns and the 1988 Montreal protocol. Other alternate fluorocarbons candidates are trifluoromethane (Freon-23), 1,1-dichloro-2,2,2-trifluoroethane (HCFC-123), 1-chloro, 1,2,2,2-tetrafluoroethane (HCFC-124), and 1,2,2,2-tetrafluoroethane (HCFC-134a). Some of these fluorocarbons may be more polarizable than Freon-22, and thus more attractive solvents. Freon-23 is of particular interest since it is non-chlorinated and presumably non-ozone depleting. Cosolvents -- ethanol,

Table 1. Thermodynamic Properties of Selected SuperFluids

Generic Name	Chemical Formula	Critical Temperature T_c (°C)	Critical Pressure P_c (MPa)	Dipole Moment (Debyes)
Carbon Dioxide	CO ₂	31.0	7.38	0.0
Nitrous Oxide	N ₂ O	36.4	4.89	0.2
Propane	C ₃ H ₈	96.6	4.25	0.1
Orthofluoropropane	C ₃ F ₈	71.9	2.68	NA*
Ethane	C ₂ H ₆	32.2	4.89	0.0
Ethylene	C ₂ H ₄	9.2	5.04	0.0
Freon-22	CHClF ₂	96.0	4.88	1.4
Freon-23	CHF ₃	25.9	4.73	1.6
HCFC-123	CF ₃ CHCl ₂	183.6	3.67	1.36
HCFC-124	CHClFCF ₃	122.2	3.62	1.47
HCFC-134a	CH ₂ FCF ₃	101.1	3.96	2.06

* Not available (the dipole moment of propane, C₃H₈, is 0.084 Debyes)

methanol, and acetone -- are used to enhance the affinity of the nonpolar and slightly polar supercritical and near-critical fluids for the solvation of phospholipids and certain pharmaceuticals.

SUPERFLUIDS SOLUBILITY OF PHOSPHOLIPIDS

In order to optimize the SFS-CFN process, the solubilities of phospholipids and other materials such as cholesterol were measured in different SFS solvents at different conditions of temperature and pressure to ensure efficient solvation of these raw materials [5]. The solubility of egg yolk phosphatidylcholine (EPC), >95% pure, in SFS propane, nitrous oxide and Freon-22 as a function of pressure at 30°C is shown in (Fig. 4).

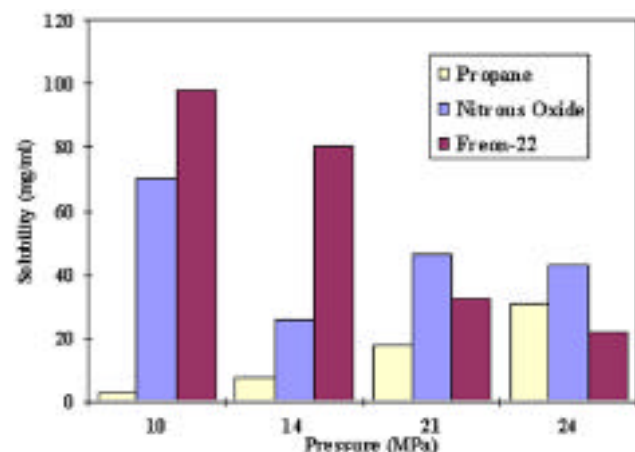


Fig. (4). Solubility of Egg Yolk Phosphatidylcholine (EPC) in SFS Propane, Nitrous Oxide and Freon-22 as a Function of Pressure at 30°C

The impact of SFS polarity on the solubility of EPC at various pressure levels is evident in Figure 4. The polarity of the three SFS is in the following order: propane, nitrous oxide and Freon-22. For a less-polar solvent, such as propane (dipole moment of 0.084 Debyes), increasing pressure increases the solubility of EPC at lower temperatures. For a more-polar SFS solvent, such as nitrous oxide (dipole moment of 0.167 Debyes), solubility decreases with increasing pressure and appears to level off around 20 MPa. When the polarity of a solvent further increases, as in the case of Freon-22 (dipole moment of 1.42 Debyes), solubility decreases more readily as pressure increases.

The solubility of EPC in SFS nitrous oxide and propane is a stronger function of temperature than pressure as respectively shown in (Fig. 5) and (Fig. 6). For nitrous oxide, EPC solubility decreases exponentially as temperature increases at all pressure levels are observed. Increasing temperature will decrease the density of SFS nitrous oxide and thus reduce its solvation power. Unlike nitrous oxide, solubility of EPC in SFS propane increases significantly with temperature at all pressure levels, especially at 14 MPa and 21 MPa, when temperature increases from 30°C to 40°C. Further increase in temperature to 50°C does not seem to have much effect on the solubility of EPC in near-critical propane.

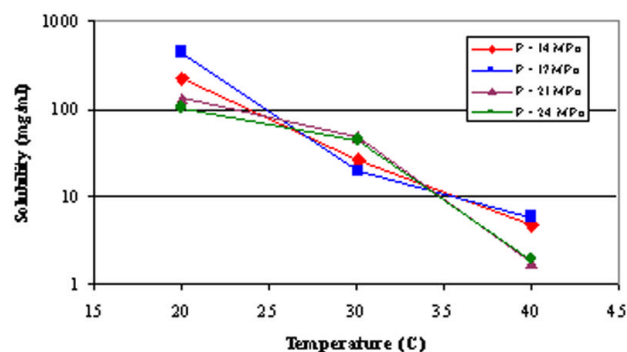


Fig. (5). Solubility of Egg Yolk Phosphatidylcholine (EPC) in SFS Nitrous Oxide

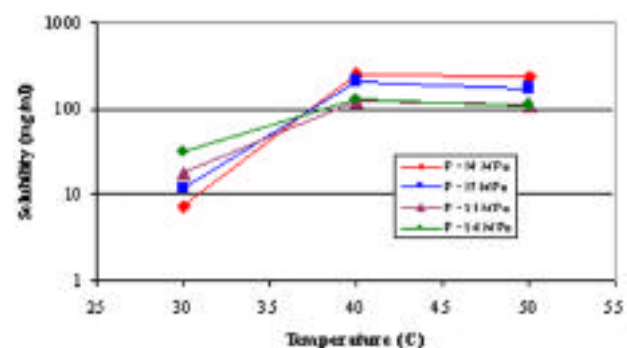


Fig. (6). Solubility of Egg Yolk Phosphatidylcholine (EPC) in SFS Propane

The solubility of hydrophobic therapeutics, such as paclitaxel, camptothecin, bryostatins 1 and betulinic acid, are usually measured in different SFS at various conditions to establish the optimal conditions for achieving targeted drug:lipid ratios in the SFS-CFN process.

CHARACTERISTICS OF PHOSPHOLIPID NANOSOMES

On the basis of mathematical modeling and semi-empirical experiments, the size and character of phospholipid nanosomes depend on the following process parameters and material properties: (i) size and design of decompression nozzle effects bubble size, and thus the size of the nanosomes formed; (2) decompressive forces that are dependent on the SFS' density, which is in turn a function of operating pressure, operating temperature and SFS type; (3) rate of decompression that defines the characteristics of the deposited phospholipid as well as the intensity of mixing and localized shear, e.g., slow decompression will produce smaller and more uniform nanosomes; (4) interfacial forces between the SFS phase and the aqueous phase which are significantly impacted by the nature and concentration of the polar entrainer used as a cosolvent; (5) charge distribution of the nanosomes and its interaction with the surrounding aqueous medium, pH, ionic strength and electrolyte composition; and (6) nature of compound being encapsulated, e.g. protein conformational structure and characteristics or degree of small molecule hydrophobicity.

Based on the conceptual model of nanosomes formation described, the number, size and characteristics of SFS nanosomes formed will be governed by the dynamics of bubble formation at a submerged capillary interface. The volumetric rate of bubble growth can be approximated by a modified version of Hagen-Poiseuille's law for the laminar flow of an incompressible fluid [6]. Assuming the portion of the bubble inside the capillary is negligible, the rate and size (R) of bubbles formation at a submerged capillary interface is governed by the following equation:

$$\frac{dR}{dt} = r^4 * \frac{[P - \rho gh - 2 \gamma / R]}{32 \mu L} \quad (1)$$

where r is the internal radius of the capillary, P is the applied pressure, ρ is the density of the liquid, h is the submerged depth of the nozzle, γ is the interfacial tension between the SFS and aqueous phase, L is the length of the capillary and μ is the viscosity of the liquid phase. In the controlled formation of single bubbles, individual bubbles will break off when the buoyancy forces equal the surface forces holding the bubble or droplet to the tube. From a force balance, the bubble size can be related to the nozzle size by the following relationship:

$$R = [(3r^3)/(2 \rho g)]^{1/3} \quad (2)$$

Equation 2 is valid for capillary tubes with a radius less than 0.01 cm (100 microns). Under these conditions, the size of bubbles and nanosomes formed by a submerged nozzle should depend on nozzle radius and interfacial tension to the one-third power. This relationship is, however, complicated by the amount of phospholipids dissolved in the SFS phase and the rate of decompression.

The impact of nozzle size on the SFS formation of nanosomes in distilled de-ionized water (DDI) was determined from SFS-CFN experiments. Nanosomes formed from a 0.5

mm nozzle with lecithin and SFS CO₂ at 28 MPa and 60°C had an average, unimodal diameter of 478 nm while nanosomes formed with a 0.06 mm nozzle and identical conditions had an average unimodal diameter of 326 nm, both as measured by a Coulter N4MD sub-micron particle size analyzer utilizing laser beam interferometry. Based on this data, the nanosome radius appears to depend on the nozzle radius to the one-fifth power. Thus, in addition to the balance between surface and buoyancy forces, the nanosomes size appears to be dependent on other variables such as applied pressure and decompressive forces.

The size of phospholipid nanosomes is dependent on operating pressure and, during batch operations, upon fractional depressurization as shown in Table 2. The larger vesicles in the last stage of fractional decompression are probably formed because the density of the SFS changes rapidly below the critical pressure and the SFS becomes more gaseous generating larger bubbles.

The stability of phospholipid nanosomes was examined by measuring particle size distribution as a function of time. No special precautions, such as preparation of the nanosomes under a blanket of inert gas, the use of antioxidants, or aseptic processing and collection procedures, were utilized. The time stability of phospholipid nanosomes at 4°C is listed in Table 3. The nanosomes were made with EPC and SFS CO₂ at 28 MPa and 60°C.

SFS CO₂ phospholipid nanosomes demonstrate excellent stability at a storage temperature of 4°C over a six-month period. Interestingly, we observed shorter destabilization times with a suspension of 310 nm Latex microspheres. Typically, we observed increases in size in as short as 10 to 20 days after storage at 4°C. Shortly thereafter, usually within 30 days of the initial preparation, contamination becomes obvious to the naked eye and the particle size changes

Table 2. Effect of Fractional SFS Depressurization on Nanosomes Size

Pressure Range (MPa)	Small		Medium		Large	
	Size (nm)	Amt (%)	Size (nm)	Amt (%)	Size (nm)	Amt (%)
SFS N ₂ O with Ethanol Co-solvent at 60°C						
21 - 14	0	0	244	100	0	0
14 - 8	0	0	295	100	0	0
8 - 0	0	0	337	56	3,140	44
SFS C ₂ H ₄ with Ethanol Co-solvent at 60°C						
21 - 14	0	0	165	100	0	0
14 - 7	0	0	183	100	0	0
7 - 0	0	0	140	76	978	24
SFS C ₃ H ₈ with Ethanol Co-solvent at 60°C						
21 - 14	0	0	120	62	1,430	38

Table 3. Time Stability of Phospholipid Nanosomes

Elapsed Time (days)	Small		Medium		Large	
	Size (nm)	Amt (%)	Size (nm)	Amt (%)	Size (nm)	Amt (%)
6	0	0	326	100	0	0
52	0	0	312	100	0	0
187	0	0	315	100	0	0

from being unimodal to bimodal with size distributions around 310 nm and 3,050 nm. Similar destabilization was observed with liposomes formed by sonication (data not shown). The stability of phospholipid nanosomes formed by supercritical carbon dioxide may thus reflect the capability of the SFS-CFN process to impart end-product sterility.

PHOSPHOLIPID NANOSOMES ENCAPSULATED CYTOCHROME-C

SFS-CFN was utilized to passively encapsulate cytochrome-C, a membrane associated protein with a molecular weight of 12,384 Daltons. The characteristics of the encapsulated cytochrome-C nanosomes and liposomes formed by sonication were evaluated by fractionating the vesicles on a Sephacryl S1000 column (Pharmacia), and measuring the particle size distributions, UV-VIS absorbance and protein content of the eluted volume fractions [1]. The encapsulation efficiency varied from 13% for liposomes formed by sonication to 33% for SFS nanosomes. Photomicrographs of SFS nanosomes formed by the controlled (slow) decompression of a SFS mixture of ethylene:ethanol, chicken egg yolk lecithin and a saline phosphate buffer containing cytochrome-C are shown in (Fig. 7).

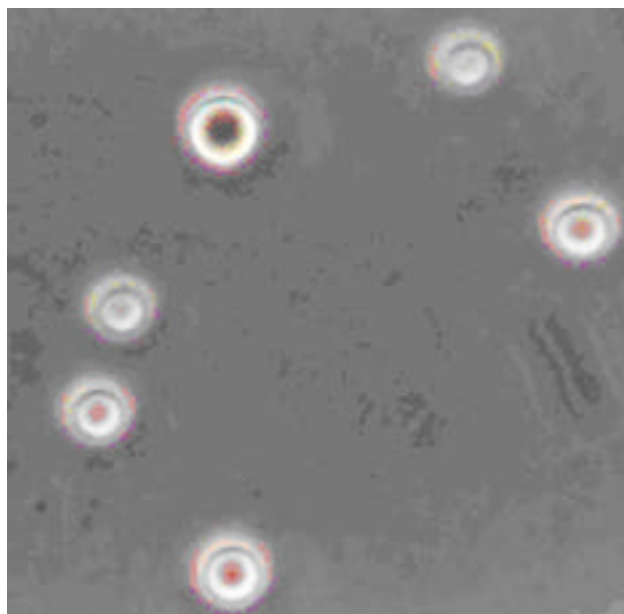


Fig. (7). Photomicrograph of Phospholipid Nanosomes Encapsulating Cytochrome-C

PHOSPHOLIPID NANOSOMES ENCAPSULATED PACLITAXEL

Paclitaxel

A diterpene plant product derived from the Pacific yew *Taxus brevifolia*, is a potent anticancer drug. It is an anti-mitotic agent that stabilizes the polymerization of tubulin and prevents rapid cell division. Paclitaxel has also shown a therapeutic efficacy as high as 62% in clinical trials for the treatment of metastatic breast cancer [7]. The efficacy of paclitaxel on a cellular level may be directly related to its very hydrophobic nature. Its formulation has been difficult because of its insolubility in most pharmaceutically acceptable solvents.

Paclitaxel is commercially formulated in 50% polyoxyethylated castor oil and 50 % dehydrated alcohol (Cremophor EL) to make Taxol . The Cremophor EL vehicle can have serious side effects including severe hypersensitivity reactions [8]. This formulation has been used for several commercially available drugs including cyclosporin, miconazole, and teniposide, and other experimental antitumor compounds such as echinomycin, didemnin B and parenteral lomustine [9]. Hypersensitivity-like reactions have been reported with all these drugs [7]. Taxol has also caused myelosuppression, peripheral neuropathy and other side effects that were dose and schedule related.

Paclitaxel Nanosomes

The raw materials utilized to produce paclitaxel nanosomes by the SFS-CFN process were phosphatidylcholine from soybean (> 95 % purity) and cholesterol (> 99 % purity). Paclitaxel (> 99 %) was manufactured from needles of the ornamental yew, *Taxus media "hicksii,"* using a supercritical fluid natural product manufacturing process [10-11]. In order to evaluate the effects of decompression pressure on nanosome size distribution, two fractional decompression experiments were conducted. These experiments (Table 4), in which the sample solution was collected over a specific pressure interval, demonstrate that nanosomes with uniform size distribution can be reproducibly obtained by properly selecting decompression pressure range and nozzle size [1-2].

Stability of Paclitaxel Nanosomes

The chemical and physical stability of paclitaxel nanosomes were evaluated at 4°C. Over the 72-day period tested, the paclitaxel concentration remained within 5% of the initial concentration and the particle size was within 3% of the initial size.

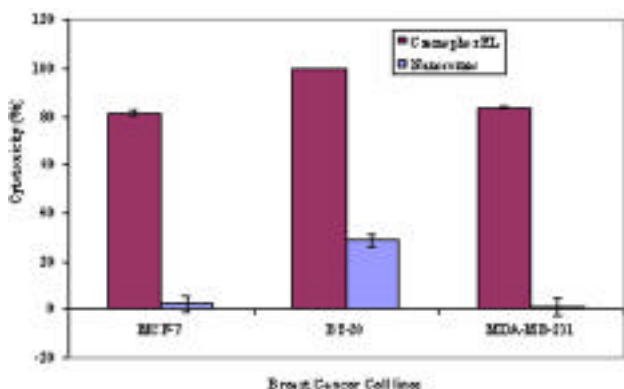
Table 4. Particle Size Analysis of Phospholipid Nanosomes Encapsulated Paclitaxel

Pressure Range (MPa)	Small		Medium		Large	
	Size (nm)	Amt (%)	Size (nm)	Amt (%)	Size (nm)	Amt (%)
24 - 6*	62	100	0	0	0	0
24 - 6**	69	100	0	0	0	0

* SFS N₂O with Ethanol Co-solvent at 60°C** SFS C₂H₄ with Ethanol Co-solvent at 60°C**In Vitro Studies with Paclitaxel Nanosomes:**

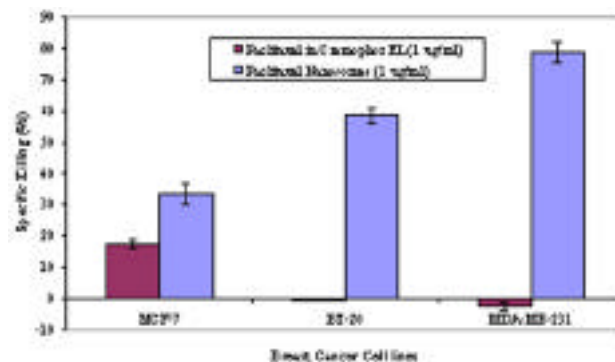
Studies were conducted on the effect of phospholipid nanosomes-encapsulated paclitaxel on human breast cancer cell lines implanted subcutaneously into nude mice. The size of the paclitaxel nanosomes was 218 nm and the paclitaxel content was 132.8 ppm. Three human breast cancer cell lines, MCF-7, BT-20 and MDA-MB-231 were used. The cells were grown in RPMI-1640 with 10% FBS, penicillin (100 µg/ml), streptomycin (100 µg/ml), and 0.3 mg/ml glutamine. There was no additional hormone supplementation. The cells were grown to approximately 80% confluency and treated with paclitaxel in Cremophor EL (Taxol), Cremophor EL alone, and paclitaxel nanosomes or nanosomes alone at a paclitaxel concentration of 1.0 µg/ml. Counts of viable cells were made using a hemocytometer.

Cremophor EL was very cytotoxic to all three breast cancer cell lines tested, (Fig. 8), while empty nanosomes were essentially nontoxic except for the BT-20 cell line in which there was about a 20% nonspecific toxicity. The phospholipid nanosomes vehicle was, as anticipated, substantially less toxic than the Cremophor EL vehicle.

**Fig. (8).** *In Vitro* Cytotoxicity of Cremophor EL and Empty Nanosomes on Different Breast Cancer Cell Lines

Paclitaxel nanosomes were much more specific than paclitaxel in Cremophor EL (Taxol) in killing breast cancer cells, (Fig. 9). The data presented is the difference between the cytotoxicity of the drug plus vehicle minus the cytotoxicity of the vehicle alone; error bars reflect the propagation of errors through the subtraction process. This data, which take into account the much higher toxicity of Cremophor EL alone over that of nanosomes alone, agree with a study [12] that suggested that Cremophor EL at high concentra-

tions was antagonistic to the action of paclitaxel. The MDA-MB-231 cell line was used in the subsequent *in vivo* studies since it appeared to be particularly susceptible to specific killing by paclitaxel nanosomes.

**Fig. (9).** *In Vitro* Specific Killing of Breast Cancer Cell Lines by Paclitaxel in Cremophor EL (Taxol) and Paclitaxel Nanosomes**In Vivo Studies with Paclitaxel Nanosomes:**

Athymic nude mice were injected subcutaneously with 10⁷ MDA-MB-231 cells. Tumors were allowed to develop at the injection site until they were approximately 100 mm³ in size. The tumor size was recorded as day 1. The mice were treated by intraperitoneal injection of saline (control), paclitaxel in Cremophor EL (Taxol), paclitaxel nanosomes and for some experiments Cremophor EL alone or empty nanosomes alone. Paclitaxel was given as a 300 µg dose in a total volume of 0.5 ml. In a second experiment, two injections were given at a two-day interval. Tumor size was measured with calipers and values for height, width, and length recorded. At sacrifice, tumors were placed in 10% formalin saline for histological examination.

A snapshot of one group of five mice used in our first *in vivo* study is shown, at the end of this study, in (Fig. 10). In mice A and A1, treated with paclitaxel nanosomes, there is no visible evidence of the tumor implanted in the right flank of mice A and some necrosis of the skin of mice A1 as a result of rapidly dying cells from killing of the tumor. In mice B with Taxol, the tumor on its right flank is as evident and about the same size as tumors on the right flank of mice C treated with empty nanosomes and mice D treated with the Cremophor EL vehicle utilized for the formulation of Taxol.

The results of a second *in vivo* study are shown in (Fig. 11). This study was simpler, but with 12 mice in each of

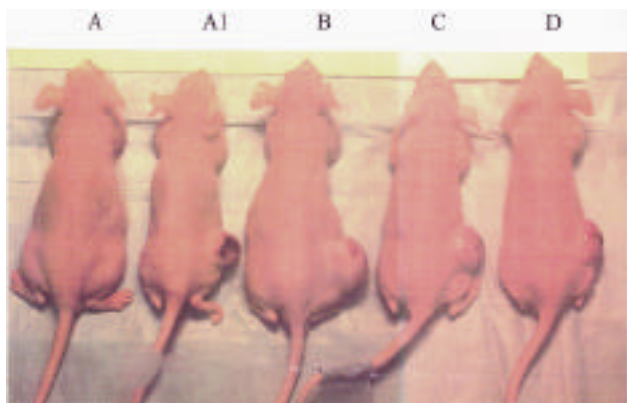


Fig. (10). Nude Mice with Breast Cancer Xenografts Treated with Paclitaxel Nanosomes [A and A1], Taxol [B], Empty Nanosomes [C] and Cremophor EL [D]

three treatment arms. These comprised of no treatment (saline injection), paclitaxel nanosomes and paclitaxel in Cremophor EL (Taxol) given intraperitoneally in two doses (total dose 24 mg/kg). This study clearly shows that paclitaxel in Cremophor EL was about 50% less effective than paclitaxel nanosomes, at the same dosing level, in inhibiting the growth of the breast cancer xenograft in nude mice.

The *in vitro* and *in vivo* results suggest that phospholipid nanosomes containing paclitaxel may be a more effective therapy against human breast cancer cell lines than the conventional anticancer therapeutic, paclitaxel in Cremophor EL (Taxol). The *in vitro* studies showed that nanosomes were much less toxic than Cremophor EL, the vehicle utilized in Taxol. The *in vivo* studies showed that paclitaxel nanosomes had a markedly greater effect on tumor growth of breast cancer xenografts than either the control group or the paclitaxel in Cremophor EL (Taxol) group.

PHOSPHOLIPID NANOSOMES ENCAPSULATED CAMPTOTHECIN

Camptothecin

Camptothecin is an antitumor alkaloid that was originally isolated from the bark and stem wood of *Camptotheca acuminata*, a small tree native to China. This compound displays unprecedented antitumor activities against leukemia, human colon cancer and a variety of solid tumor systems. In particular, camptothecin was discovered to trap the cleavable complex between topoisomerase I and DNA [13]. Camptothecin is a unique topoisomerase I inhibitor which, while very effective, is not yet completely understood. In addition, camptothecin inhibits the replication of HIV and other viruses.

Camptothecin full therapeutic activity has been limited by poor water solubility and the aqueous instability of the lactone ring moiety. Ring opening will cause loss of biological activity of this compound. Preferential binding of the biologically inactive carboxylate form with human serum albumin further hinders drug effectiveness [14]. Administration of the soluble sodium salt of camptothecin has proved to be ineffective and delayed the development of this potent anticancer compound. As a result of this, camptothecin analogs that exhibit a superior solubility profile while retaining antitumor activity have been developed. These goals are frequently at odds, as increased hydrophilicity engenders greater exposure to the deactivating aqueous environment [15]. Several clinical candidates, such as topotecan, CPT-11, and 9-aminocamptothecin, have been developed [16]; topotecan and CPT-11 have been approved by the United States FDA for colorectal and other cancers.

Water-soluble camptothecin analogs may not be as effective as the native compound and some of its hydrophobic analogs. For example, researchers [17] have reported on the *in vivo* activity of two water soluble camptothecin analogs. Even at the maximum active dose, no cures were obtained.

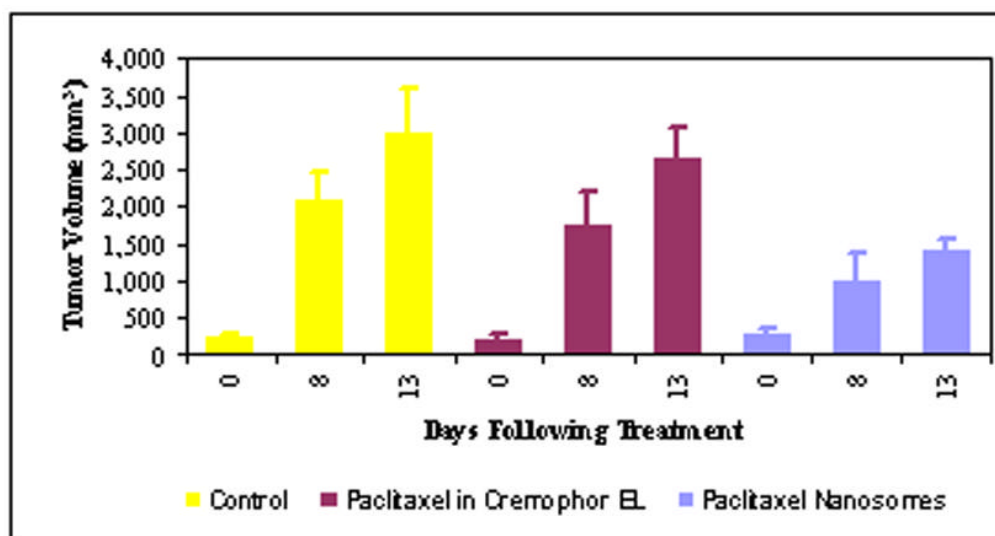


Fig. (11). *In Vivo* Efficacy of Paclitaxel Nanosomes, Paclitaxel in Cremophor EL (Taxol) and Saline Injections on Breast Cancer Growth in Nude Mice

This may be due to the instability of the lactone pharmacophore in aqueous media in general and in plasma in particular, the latter due at least in part to binding with human serum albumin. Nanosome encapsulated camptothecin can potentially serve as a useful drug delivery system for solubilizing camptothecin, while retaining both its lactone ring and antitumor activity.

Camptothecin Nanosomes

Utilizing the SFS-CFN injection technique, camptothecin was encapsulated into stable, uniform nanosomes. Soy phosphatidylcholine and cholesterol were the nanosomal raw materials utilized. Solvation conditions were 3,000 psig and 40°C with near-critical propane. Following decompression, the nanosomal solution was centrifuged at 5,000 rpm for 10 minutes, and the supernatant passed 5 times through a 100 nm polycarbonate filter. The Coulter Submicron Particle Analyzer confirmed a size distribution centered at 100 nm (S.D. 35 nm). Camptothecin concentration of the nanosomal solution produced was measured to be 1.1 mg/ml by HPLC analysis.

Anticancer Activity of Camptothecin Nanosomes

The United States National Cancer Institute conducted *in vivo* testing of camptothecin nanosomes. Ten mice were implanted with lymphoma xenografts and given intravenous treatment. For the lowest dose/schedule tested, five were found to be tumor-free (cured) after 69 days. This high level of activity suggests that phospholipid nanosomes encapsulated camptothecin will improve efficacy, reduce toxicity while improving solubility and stability of this unique topoisomerase I inhibitor and anticancer drug.

PHOSPHOLIPID NANOSOMES ENCAPSULATED BETULINIC ACID

Betulinic acid (Fig. 12a), a pentacyclic triterpene, and its precursor, betulin (Fig. 12b), are components of the bark of the *Betula alba* (white birch) tree. The tree is fast growing and abundant in North America and Europe. The raw material is readily available in large quantities since birch bark is considered a waste product in the pulp and paper, and furniture manufacturing industries.

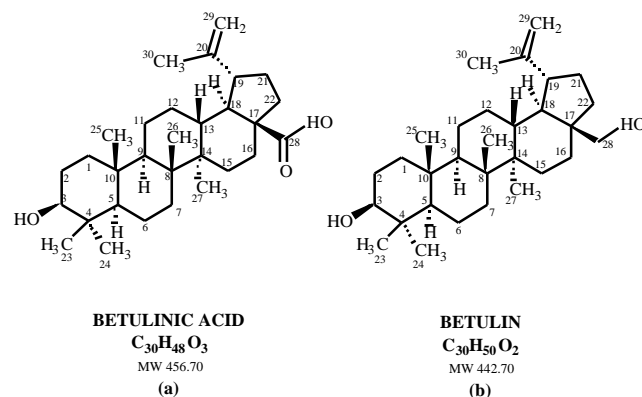


Fig. (12). Chemical Structures, Formulae and Molecular Weights of Betulin and Betulinic Acid

Anticancer Activity of Betulinic Acid

Betulinic acid has demonstrated cytotoxic activity specific for melanoma cells both *in vitro* and *in vivo*. *In vitro*, this melanoma-specific cytotoxicity occurs through apoptosis; however, this mechanism is not well understood. When administered intraperitoneally to athymic mice bearing human melanoma xenografts, betulinic acid is concentrated in the tumors, resulting in rapid tumor regression with no observable toxicity to the animal even at high doses (e.g., 500 mg/kg body weight, i.p.). Direct injection of betulinic acid into the tumor of xenografts induced apoptosis within the tumors [18].

Anti-Infective Activity of Betulinic Acid and its Derivatives

Betulinic acid has also been shown to have potent anti-HIV activity by a novel mechanism of action, with an EC_{50} (50% effective concentration) of 1.4 μ M and a therapeutic index (toxicity divided by efficacy) of 9.3 [19]. In addition to preventing entry of HIV into the target cell, it may also act at the maturation stage. Problems have been encountered, as betulinic acid is insoluble in many solvents. Derivatives of betulinic acid have been made and tested to circumvent this problem. Panacos Pharmaceuticals, Baltimore, MD has recently put a betulinic acid derivative [PA-457 or 3-O-(3',3'-dimethylsuccinyl) betulinic acid] into Phase I clinical trials for HIV. PA-457 disrupts the late-stage viral maturation processes of HIV's *gag* protein. The *gag* protein forms the capsid shell around a retrovirus' RNA and establishes a viral core structure. Treatment with PA-457 causes this core structure to be defective and non-infectious. Betulinic acid and its derivatives have also demonstrated anti-infective activity against herpes virus [20], malaria [21] and leishmaniasis [22].

Betulinic Acid Nanosomes

The nanosomes raw materials utilized for the phospholipid nanoencapsulation of betulinic acid were DMPC, a synthetic saturated phosphatidylcholine that was purchased from Avanti Polar Lipids, Alabaster, AL (Catalog No. 850345) and DMPG, a synthetic saturated phosphatidylglycerol that was purchased from Avanti Polar Lipids, Alabaster, AL (Catalog No. 840445). DMPC has a Molecular Weight of 677.95, a transition temperature of 23°C and a zero net charge at pH of 7.4. DMPG has a Molecular Weight of 688.85. The targeted drug:lipid ratio was DMPC:DMPG:Betulinic Acid::21:9:1.

Phospholipid nanosomes encapsulated betulinic acid were prepared using the B operating mode in the SFS-CFN apparatus, (Fig. 3). *SuperFluids* Freon-22 at 21 MPa and 40°C was utilized to form the betulinic acid nanosomes, primarily because it has a solubility of ~ 0.025 mg/ml in Freon-22 at these conditions. Alternatively, we could have utilized *SuperFluids* CO₂:ethanol::60:40 at 21 MPa and 40°C that would have required ten times more betulinic acid since its solubility of betulinic acid is ~ 0.25 mg/ml.

The betulinic acid nanosomes made in a 10% sucrose solution had a unimodal particle size distribution with a mean diameter of 180 nm ranging from 174 to 186 nm (95%

confidence limits) and, by HPLC analysis, contained 12.5 µg/ml betulinic acid. After freeze-drying and re-suspension in de-ionized water, the mean diameter increased slightly to 202 nm and the betulinic acid content decreased slightly to 11.1 µg/ml. In a subsequent SFS-CFN experiment, betulinic acid nanosomes were formed in a 1% sucrose solution in order to increase the drug concentration by 10-fold after freeze-drying and re-suspension. The initial product had an average unimodal mean diameter of 186 nm and contained 18.6 µg/ml betulinic acid. After freeze-drying and re-suspension in de-ionized water by a concentration of 12, the average unimodal mean diameter increased to 235 nm and the betulinic acid content increased significantly to 87.7 µg/ml.

A nanosomal formulation run was performed with the phospholipid raw materials but without betulinic acid. The conditions for this run were identical to that of the betulinic acid nanosomes run. This nanosomal formulation, also in a 1% sucrose solution, served as a vehicle control in subsequent bioactivity assays.

Anti-HIV Activity and Cytotoxicity

Several experiments were conducted to evaluate the anti-HIV activity of betulinic acid nanosomes made utilizing SFS-CFN and compare that with the anti-HIV activity of non-encapsulated betulinic acid.

A stock solution of the betulinic acid standard at 10 mg/ml was prepared in dimethyl sulfoxide (DMSO). Serial 1:2 or 1:5 dilutions were tested in triplicate in the anti-HIV assay, described below, beginning with 100 µg/ml. The same batch of betulinic acid was used to prepare the nanosomal formulation of betulinic acid in a 1% sucrose solution. The nanosomes, with a betulinic acid concentration of 18.6 µg/ml, was filtered through a 0.2 µm low protein-binding filter and serial 1:2 or 1:4 dilutions were tested in triplicate beginning with 9.3 µg/ml of betulinic acid. A sample of the empty nanosomes was also filtered through a 0.2 µm low protein binding filter and serial 1:2 dilutions were tested in triplicate beginning with the 1:2 dilution.

Viral reduction assays were performed to determine and quantify the presence of anti-HIV activity in the samples. Briefly, 100 TCID₅₀ (50% tissue culture infectious dose) of HIV_{IIB} was incubated with CEM-SS cells for 1 hour at 37°C. Upon removal of the virus, serial dilutions of the sample, 3TC, or media were added and the cells incubated at 37°C. On day 3, most of the media was replaced with fresh media with or without the diluted sample or 3TC. On day 7, supernatant was collected and the amount of p24 assayed by ELISA (SAIC-Frederick). 3TC, known inhibitors of HIV, were used as a positive control for p24 reduction. Wells lacking virus served as a negative control for virus infection while wells containing virus, but no sample/drug, served as a positive control for virus infection. The percent p24 reduction was determined by the following equation: $(((\text{cells} + \text{virus}) - (\text{cells} + \text{virus} + \text{test item})) / (\text{cells} + \text{virus})) * 100$. When possible, the 50% effective concentration (EC₅₀) was determined.

Additionally, a cytotoxicity assay was performed with the samples. Briefly, serial 1:2 dilutions of samples was

added to 50,000 CEM-SS cells per well of a 96-well plate and allowed to incubate at 37°C for 7 days. On day 3, 150 µl/well of spent media were replaced with media or diluted samples. After the incubation a viability dye, WST-1, was added and the plate incubated for 1 hour. After shaking the plate for 1 minute, it was read in a microplate reader at 450 nm with a reference of 630 nm. Controls included media alone, cells alone, as well as dilutions of DMSO and 1% sucrose that were present in the betulinic acid and nanosomal formulation samples, respectively. After subtraction of the background (media alone wells), the percent toxicity was calculated from the following: $(((\text{cells} + \text{media}) - (\text{cells} + \text{sample})) / (\text{cells} + \text{media})) * 100$. The 50% cytotoxic concentration (CC₅₀) was then determined. Finally, the selective index (SI), which is a ratio of CC₅₀ to EC₅₀, was determined.

In an *in vitro* cytoprotection assay, betulinic acid inhibited p24 production by 76% at 20 µg/ml, (Fig. 13); the EC₅₀ was 6.72 µg/ml or 14.7 µM. The positive control 3TC resulted in 93% inhibition of p24 production at 0.2 µM, as expected. The nanosomal formulation of betulinic acid inhibited p24 production by 73% at 2.3 µg/ml; the EC₅₀ was 1.01 µg/ml or 2.2 µM (based on betulinic acid content). A second assay confirmed these results, showing that betulinic acid nanosomes inhibit HIV at lower concentrations than betulinic acid alone, and that the empty nanosomes have a minimal effect on HIV. Given the consistent results obtained with the positive control, these experiments suggest that the nanosomal formulation, produced by SFS-CFN, enhances the natural properties of the nanoencapsulated betulinic acid.

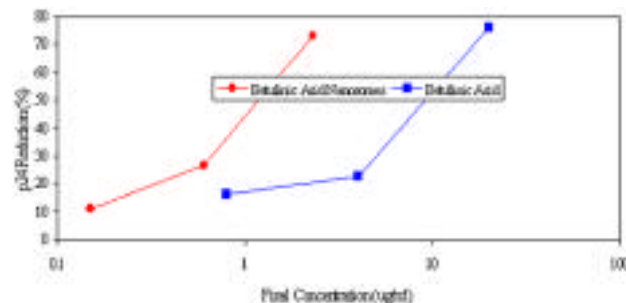


Fig. (13). Inhibition of HIV p24 by Neat Betulinic Acid and Nanosomal Betulinic Acid

CONCLUSIONS

Phospholipid nanosomes can be used for the encapsulation and improved drug delivery of protein macromolecules, nucleic acids and other hydrophilic drugs, as well as hydrophobic therapeutics such as anticancer and anti-HIV drugs. The nanosomes are manufactured by a supercritical fluid process that does not utilize organic solvents such as chloroform. In traditional rotary evaporation techniques, chloroform may be deleterious to the encapsulated therapeutics and phospholipid raw materials. The phospholipid nanosomes process substitutes supercritical, critical or near-critical fluid solvents with or without polar cosolvents such as ethanol for organic solvents utilized to solvate phospholipid raw materials.

The SFS-CFN process, for manufacturing phospholipid nanosomes, also replaces the shear generated by sonication

and high-pressure homogenization with decompressive forces. For the SFS utilized, the maximum pressure requirements are around 3,000 to 5,000 psig because both effects of decompressive energy and phospholipid solubility should reach points of diminishing returns beyond a reduced pressure (operating pressure divided by critical pressure) of about 3.0. These pressure requirements are significantly lower than those of high-pressure homogenization, reducing equipment wear and operating costs.

The process does not generate excessive heat that can damage thermally labile proteins and phospholipids. Unlike high-pressure homogenization that can result in the generation of local hot spots by the dissipation of pressure and shear energy within the microchannels of the homogenizing valve, the SFS-CFN process produces a cooling effect as a result of Joule-Thompson effects generated during decompression. This cooling effect can be designed to freeze multilamellar vesicles (MLVs), and the subsequent formation of FATMLVs (freeze and thawed multi-lamellar vesicles) with the added benefits of higher loading efficiencies and slower drug release rates.

The process has several degrees of freedom such as nozzle diameter and size, operating pressure and temperature, type and concentration of SFS solvents as well decompression rates and manufacturing technique. The decompression technique, like high pressure homogenization, can be used to form small unilamellar vesicles (SUVs). The injection technique, which is more like the rotary evaporation and sonication techniques, can be used to form SUVs, LUVs (large unilamellar vesicles), MLVs and FATMLVs. The evaporation technique can be used to readily encapsulate hydrophobic drugs. With all three techniques, the SFS mixture can be decompressed through a filter to decrease nanosome size, improve uniformity and, with 0.22-micron filters, enhance sterility.

The SFS-CFN process is a single-step one increasing speed of processing versus the multiple pass requirements of high-pressure homogenization. The process can be operated in a continuous mode because it is a single step-one, and the primary solvent can be readily separated, recovered and reused. The SFS-CFN manufacturing techniques are scalable because they are essentially liquid-liquid unit operations, and may impart an enhanced degree of end-product sterility since supercritical fluid technologies will disrupt and inactivate microbial and viral pathogens [23-27].

Phospholipid nanosomes could lead to an increase in a drug's therapeutic index resulting in: (i) enhanced therapeutic efficacy; (ii) elimination of pre-medication to counteract vehicles such as Cremophor EL; (iii) reduction of drug toxicity side effects; (iv) prolonged circulation time and increased therapeutic effect; and (v) improved quality of life.

ACKNOWLEDGEMENTS

This research was, in part, supported by grants and contracts from the United States National Science Foundation

(Grants No. ISTI-8961217 and ISTI-9112190) and the United States National Cancer Institute, National Institutes of Health (Grant No. 1R43-CA-58140, and Contracts No. N43-CM-17019 and N44-CM-27122).

REFERENCES

- [1] Castor, T.P. U.S. Patent No. 5,554,382, **1996**; European Patent No. 0,703,778, **1997**.
- [2] Castor, T.P.; Chu, L. U.S. Patent No. 5,776,486, **1998**; European Patent No. 0,792,143, **2002**.
- [3] Castor, T.P.: Supercritical Fluid Liposome Formulations presented at a symposium entitled Liposomes and Vesicles: Fundamentals and Applications at AIChE Annual Meeting, San Francisco, CA, **1994**.
- [4] Reid, R.C.; Praustnitz, J.M.; Sherwood, T.K. *The Properties of Gases and Liquids*, McGraw-Hill Book Company, New York, **1977**.
- [5] Chu, L.; Laska, M.; Berrien, L.S.; Castor, T.P. *Solubility of Phospholipids in Supercritical Fluids* presented at the 12th Symposium on Thermophysical Properties, Boulder, CO, **1994**.
- [6] Bird, R.B.; Stewart, W.E.; Lightfoot, E.N. *Transport Phenomena*, John Wiley & Sons, Inc., New York, **1960**.
- [7] Holmes, F.A.; Walters, R.S.; Theriault, R.L.; Forinan, A.D.; Newton, L.K.; Raber, M.N. *Journal of National Cancer Institute*, **1991**, 83(24), 1797-1805.
- [8] Rowinsky, E.K.; Donehower, R.C. *Journal of National Cancer Institute*, **1991**, 83(24), 1778-81.
- [9] Arbuch, S.G.; Canetta, R.; Onetto, N.; Christian, M.C. *Seminars in Oncology*, **1993**, 20(4, suppl. 3), 31-9.
- [10] Castor, T.P. U.S. Patent 5,750,709, **1998**.
- [11] Castor, T.P. U.S. Patent No. 5,440,055, **1995**; European Patent No. 0,689,537, **1997**; Chinese Patent No. ZL 94 1 91805.X, **2000**; Korean Patent No. 10-311330, **2002**; Japanese Patent No. 3,478,341, **2003**.
- [12] Liebmann, J.E.; Cook, J.A.; Lipschultz, C.; Teague, D.; Fisher, J.; Mitchell, J.B. *Br. J. Cancer*, **1993**, 68, 104-9.
- [13] Hertzberg, R.P.; Caranfa, M.J.; Hecht, S.M. *Biochemistry*, **1989**, 28, 4629-38.
- [14] Burke, T.G.; Mi, Z.J. *Medicinal Chemistry*, **1994**, 37, 40-6.
- [15] Burke, T.G.; Mishra, A.K.; Wani, M.C.; Wall, M.E. *Biochemistry*, **1993**, 32, 5352-64.
- [16] Potmesil, M. *Cancer Research*, **1994**, 54, 1431-9.
- [17] Emerson, D.L.; Besterman, J.M.; Brown, H.R.; Evans, M.G.; Leitner, P.P.; Luzzio, M.J.; Shaffer, J.E.; Sternbach, D.D.; Uehling, D.; Vuong, A. *Cancer Research*, **1995**, 55, 603-9.
- [18] Pezzuto, J.M.; Das Gupta T.K.; Kim, D.S.H.L. *U.S. Patent No. 5,869,535*, **1999**.
- [19] Lee, K-H.; Kashiwada, Y.; Hashimoto, F.; Cosentino, L.M.; Manak, M. *U.S. Patent No. 5,679,828*, **1997**.
- [20] Carlson, R.M.; Krasutsky, P.A.; Karim, R. *U.S. Patent No. 5,750,578*, **1998**.
- [21] Bringmann, G.; Saeb, W.; Assi, L.A.; Francois; G.; Narayanan, S.S.; Peters, K.; Peters, E-M. *Planta Med.*, **1997**, 63, 255.
- [22] Chowdhury, A.R.; Mandal, S.; Goswami, A.; Ghosh, M.; Mandal, L.; Chakraborty, D.; Ganguly, A.; Tripathi, G.; Mukhopadhyay, S.; Bandyopadhyay, S.; Majumder, H.K. *Molecular Medicine*, **2003**, 24.
- [23] Lin, H-M.; Yang, Z.; Chen, L-F. *Biotechnology Progress*, **1992**, 8, 458-61.
- [24] Castor, T.P.; Lander, A.D. U.S. Patent No. 6,465,168, **2002**.
- [25] Castor, T.P.; Lander, A.D. European Patent No. 0,629,135, 2000; Great Britain Patent No. 0,629,135, 2000; French Patent No. 0,629,135, 2000; Austrian Patent No. E194,921, 2001; German Patent No. 69,329,108.7-08, **2001**.
- [26] Castor, T.P.; Lander, A.D.; Cosman, M.D.; d'Entremont, P.R.; Pelletier, M.R. *U.S. Patent No. 5,877,005*, **1999**.
- [27] Castor, T.P.; Hong, G.T. U.S. Patent No. 5,380,826, **1995**.